


 CrossMark  
 click for updates

 Cite this: *RSC Adv.*, 2016, 6, 113016

# The interaction between CuO and Al<sub>2</sub>O<sub>3</sub> and the reactivity of copper aluminates below 1000 °C and their implication on the use of the Cu–Al–O system for oxygen storage and production†

 Wenting Hu,<sup>‡\*ab</sup> Felix Donat,<sup>bc</sup> S. A. Scott<sup>a</sup> and J. S. Dennis<sup>b</sup>

The reversible decomposition of CuO into Cu<sub>2</sub>O and oxygen at high temperature, typically between 850 and 1000 °C, provides a means of separating pure oxygen from air. In such a process, the oxide generally has to be supported on a refractory oxide, e.g. alumina, to maintain its capacity when cycled many times between CuO and Cu<sub>2</sub>O. One problem is that if the CuO reacts with the alumina to form CuAl<sub>2</sub>O<sub>4</sub>, the latter releases oxygen too slowly to be of practical use so that the capacity for oxygen release of such a carrier falls progressively as more aluminate is formed. However, the reported temperatures at which CuAl<sub>2</sub>O<sub>4</sub> forms are inconsistent so far. This work sets out to investigate the interaction between CuO and different aluminas (and precursors), which are commonly used as support materials, at temperatures between 700 and 1000 °C, as well as some chemical properties of the resulting copper aluminates. It was found that the formation of CuAl<sub>2</sub>O<sub>4</sub> occurred at around 700 °C, 800 °C and 950 °C, when amorphous aluminium hydroxide, γ-alumina, and α-alumina were used as the source of alumina support, respectively. The decomposition of CuAl<sub>2</sub>O<sub>4</sub> in an oxygen-lean environment can lead to the formation of α-alumina as well as γ-alumina, depending on the partial pressure of oxygen. Given that the α-form does not react with CuO around 900 °C, the typical operating temperature for the CuO/Cu<sub>2</sub>O couple, this observation can be used to partially regenerate CuO from CuAl<sub>2</sub>O<sub>4</sub>, for oxygen storage and production at this temperature by decomposing the spinel in a controlled atmosphere to form only α-alumina. However, during the decomposition of CuAl<sub>2</sub>O<sub>4</sub>, delafossite CuAlO<sub>2</sub> is also formed, limiting the amount of Cu that could be recovered as CuO in a single process cycle.

Received 11th September 2016

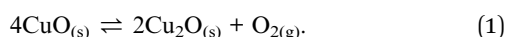
Accepted 21st November 2016

DOI: 10.1039/c6ra22712k

[www.rsc.org/advances](http://www.rsc.org/advances)

## 1. Introduction

CuO is an attractive candidate for the production of oxygen at temperatures around 900 °C owing to its suitable thermodynamic equilibrium as well as the high capacity for the release of gaseous oxygen in



<sup>a</sup>Department of Engineering, University of Cambridge, Trumpington Street, Cambridge, CB2 1PZ, UK. E-mail: [wenting.hu@newcastle.ac.uk](mailto:wenting.hu@newcastle.ac.uk)

<sup>b</sup>Department of Chemical Engineering and Biotechnology, University of Cambridge, Pembroke Street, Cambridge, CB2 3RA, UK

<sup>c</sup>Laboratory of Energy Science and Engineering, Department of Mechanical and Process Engineering, ETH Zürich, 8092 Zürich, Switzerland

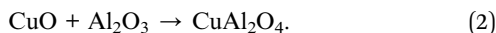
† Electronic supplementary information (ESI) available. See DOI: 10.1039/c6ra22712k. All data accompanying this publication are directly available within the publication or within the accompanying ESI; raw datafiles are available at <https://www.repository.cam.ac.uk>; <https://doi.org/10.17863/CAM.6486>

‡ Present address: Merz Court, School of Chemical Engineering and Advanced Materials, Newcastle University, Newcastle upon Tyne, NE1 7RU, UK.

The stoichiometric yield of oxygen is about 10 wt% of the CuO. The forward reaction can take place in an oxygen-lean atmosphere, e.g. pure CO<sub>2</sub> or steam, and the gaseous oxygen produced (mixed with CO<sub>2</sub> or steam) used to burn a solid carbonaceous fuel instead of air. As a result, the dried gaseous products of combustion are largely free of non-condensable gases such as N<sub>2</sub> and consist primarily of CO<sub>2</sub>, which can be subsequently sequestered with minimal treatment and separation.<sup>1,2</sup> The Cu<sub>2</sub>O produced can be oxidised in air to re-form CuO for repeated use. It is possible to arrange for the combustion of the solid fuel to occur *in situ* with the oxide releasing oxygen in accordance with the forward reaction of (1) and with the regeneration of CuO taking place in a separate reactor free of fuel. Such a scheme is termed chemical-looping with oxygen uncoupling (CLOU)<sup>3</sup> and has been demonstrated in continuous operation with different fuels at various scales.<sup>4–6</sup> Alternatively, the combustion can be conducted in a separate combustor, in which case reaction (1) serves as an air separation step. This is known as chemical-looping air separation (CLAS)<sup>7</sup> and replaces the energetically-demanding cryogenic separation of oxygen commonly proposed for oxy-fuel combustion.

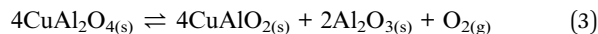


In practice, pure CuO sinters at temperatures as low as 800 °C (ref. 8) and must be supported on refractory materials with high melting points to retain its reactivity for repeated redox cycles. Al<sub>2</sub>O<sub>3</sub> is a popular choice of refractory because of its abundance and low cost: many copper-based oxygen carriers have been developed with it.<sup>9–13</sup> Depending on the method of synthesis, it is possible for CuO and Al<sub>2</sub>O<sub>3</sub> to form the spinel CuAl<sub>2</sub>O<sub>4</sub>:



The spinel is relatively stable to decomposition. It is therefore important to investigate whether the interaction of CuO and Al<sub>2</sub>O<sub>3</sub> can be inhibited at temperatures around 900 °C to preserve the capacity for oxygen transfer due to reaction (1). The current understanding of the Cu–Al–O system appears incomplete. Firstly, no consistent conclusion has been reached with regard to the lowest temperature at which the formation of CuAl<sub>2</sub>O<sub>4</sub> becomes appreciable. Secondly, and importantly, it is still unclear whether CuAl<sub>2</sub>O<sub>4</sub>, once formed, can be decomposed readily into the constituent oxides to restore the capacity for oxygen release. The objective of this paper is to address these two issues, with a particular focus on their relevance to chemical-looping processes for oxygen storage and production.

Amongst previous investigations, Jacob and Alcock<sup>14</sup> showed that CuAl<sub>2</sub>O<sub>4</sub> is thermodynamically stable in air at temperatures above ~600 °C and remains so until at least 1000 °C, depending on whether CuO or Al<sub>2</sub>O<sub>3</sub> is in excess. Misra and Chaklader<sup>15</sup> reported the formation of CuAl<sub>2</sub>O<sub>4</sub> from mechanically-mixed fine powders of CuO and abrasive alumina at 800 °C but not at 700 °C. De Diego *et al.*<sup>9</sup> impregnated a porous  $\gamma$ -alumina substrate with a solution of Cu(NO<sub>3</sub>)<sub>2</sub>, followed by decomposition of the nitrate at 550 °C for 30 minutes and subsequent calcination in air between 550 °C and 950 °C for 1 hour. The presence of CuAl<sub>2</sub>O<sub>4</sub> was observed in particles calcined at 850 °C or above but not in those calcined at <800 °C. Interestingly, after the particles were subjected at 800 °C to 100 cycles consisting of reduction to metallic Cu with CH<sub>4</sub> and re-oxidation with air, CuAl<sub>2</sub>O<sub>4</sub>, as well as  $\alpha$ -alumina, were detected in all of them regardless of the calcination temperature used to make the particles originally. Imtiaz *et al.*<sup>12</sup> found that a significant amount of CuAl<sub>2</sub>O<sub>4</sub> was formed after co-precipitates of copper and aluminium hydroxides, produced from their respective nitrates and NaOH, were fired at 800 °C for 2 hours. On the other hand, the freeze-granulated particles produced from powders of CuO and  $\alpha$ -alumina studied by Arjmand *et al.*<sup>11</sup> only formed a small amount of CuAl<sub>2</sub>O<sub>4</sub> after being calcined at 950 °C for 6 hours, despite having a ratio of Cu : Al much closer to the stoichiometry of CuAl<sub>2</sub>O<sub>4</sub> in the starting mixture. Whilst the spinel can be reduced rapidly to metallic Cu and Al<sub>2</sub>O<sub>3</sub> in the presence of reducing gases such as CH<sub>4</sub> and H<sub>2</sub> (ref. 9–11 and 16–18) at temperatures around 900 °C, the decomposition of CuAl<sub>2</sub>O<sub>4</sub> in an inert environment is rather slow<sup>11,12</sup> and therefore unsuitable for the production of oxygen. Interestingly, the equilibrium partial pressure of O<sub>2</sub> ( $P_{\text{O}_2}$ ) in



is 0.014 bar at 900 °C, similar to that of reaction (1), 0.016 bar, at the same temperature. Moreover, if excess CuO is present, the production of oxygen can take place *via* the solid–solid reaction



with an equilibrium partial pressure of O<sub>2</sub> of 0.048 bar.<sup>14</sup> Thus the much slower rate of decomposition of CuAl<sub>2</sub>O<sub>4</sub> in comparison to CuO is probably due to chemical kinetics rather than thermodynamics.

Of course, one strategy to avoid interaction between CuO and alumina would be to utilise other types of support. For instance, MgAl<sub>2</sub>O<sub>4</sub> (ref. 11, 12 and 19–21) or calcium aluminates, either in the form of commercial cement<sup>22</sup> or synthesised from pure materials,<sup>23,24</sup> have shown promising performance. However, given that the impregnation of commercial alumina catalyst support is a very convenient method for preparing copper-based carriers, the formation of the spinel merits attention.

## 2. Experimental

### 2.1. Preparation of materials

Materials with a nominal composition of 70 wt% CuO and 30 wt% Al<sub>2</sub>O<sub>3</sub> were prepared by mechanical mixing. An appropriate amount of  $\alpha$ -alumina powder (Sigma-Aldrich,  $\geq 98\%$ ), crushed  $\gamma$ -alumina pellets (originally 3 mm spheres, Alfa Aesar) or powdered Al(OH)<sub>3</sub> (Sigma-Aldrich, 50–57% on Al<sub>2</sub>O<sub>3</sub> basis) was mixed with CuO powder (Sigma-Aldrich,  $\geq 98\%$ ) in a planetary ball mill (MTI, MSK-SFM-1) operating at 25 Hz for 2 hours to produce a homogeneous mixture. The resulting mixture was calcined in air for 6 hours at a known, constant temperature between 600 °C and 1000 °C for various samples, in a box furnace. For some materials, in particular those containing  $\alpha$ -alumina, the milling and calcination process was repeated up to 4 times. These materials are named in a systematic way for easy identification. For instance, a-Al30Cu70-1000-4 denotes the material prepared from  $\alpha$ -alumina (g – for  $\gamma$ -alumina and h – for Al(OH)<sub>3</sub>) and calcined at 1000 °C, 4 times.

In addition, CuAl<sub>2</sub>O<sub>4</sub> was synthesised as follows. A 1.0 M solution of NH<sub>4</sub>HCO<sub>3</sub> (Fisher Scientific, 99%) was gradually added to 200 mL of a stirred solution containing 0.10 M Cu(NO<sub>3</sub>)<sub>2</sub> (Sigma-Aldrich,  $\geq 98\%$ ) and 0.20 M Al(NO<sub>3</sub>)<sub>3</sub> (Fisher Scientific,  $\geq 98\%$ ) until pH 4.0 was reached. The resulting gel was dried at 80 °C overnight and calcined in air at 1000 °C for 6 hours in a box furnace. The solid obtained was subsequently crushed and sieved to <50  $\mu\text{m}$  and 50–100  $\mu\text{m}$  for phase identification and thermogravimetric (TG) analysis, respectively.

### 2.2. Characterisation of materials

The phases present in the prepared materials were identified from X-ray powder diffraction (XRD; Empyrean PANalytical, Cu-K $\alpha$ , 40 kV, 40 mA) in the range  $2\theta = 5\text{--}80^\circ$  with a step size of  $0.0167^\circ$ . The references used for phase identification were: ICSD-31701 (CuAlO<sub>2</sub>), ICSD-172145 (CuAl<sub>2</sub>O<sub>4</sub>), ICSD-52043 (Cu<sub>2</sub>O), ICSD-16025 (CuO), ICSD-64699 (Cu), ICSD-99836



(tetragonal  $\gamma$ -alumina), ICSD-82504 ( $\theta$ -alumina) and ICSD-31545 ( $\alpha$ -alumina). The reactivity of various materials was characterised using a thermogravimetric analyser (TGA; Mettler Toledo, TGA/DSC1). The TGA furnace was always purged by two streams of Ar (BOC, >99.998%) at a total flowrate of 100 mL  $\text{min}^{-1}$  in addition to a stream of reactive gas with a flowrate of  $\sim 50$  mL  $\text{min}^{-1}$ . The flowrates are as measured at 20  $^{\circ}\text{C}$  and atmospheric pressure, and this applies to all flowrates quoted in the following text, unless specified otherwise. The reactive gas could be switched between air (BOC, >99.995%),  $\text{N}_2$  (BOC, >99.998%) or 5 vol%  $\text{H}_2$  balanced by  $\text{N}_2$  (BOC, >99.999%; referred to simply as  $\text{H}_2$  hereafter) using a solenoid valve manifold (Bürkert, type 6011) controlled from a separate program synchronised with the TGA.

Two types of TG experiments were undertaken on fresh materials. In the first, to quantify the total amount of Cu (on a CuO basis) and  $\text{CuAl}_2\text{O}_4$  present in the prepared materials, approximately 20 mg of powdered sample was subjected to isothermal reaction at 900  $^{\circ}\text{C}$  with a reactive gas sequence air– $\text{N}_2$ – $\text{H}_2$ –air, each lasting 15 minutes. In the second, to investigate the reactivity of pure  $\text{CuAl}_2\text{O}_4$ , approximately 20 mg of the synthesised samples were held at 1000  $^{\circ}\text{C}$ , initially in air. Once the temperature and the mass of the sample had stabilised, the atmosphere was switched to a mixture of air and  $\text{N}_2$ , resulting in a partial pressure of  $\text{O}_2$  ranging from 0–0.02 bar for 50 minutes. It should be noted that when no air was used, the partial pressure of  $\text{O}_2$  in the TGA furnace was  $<5 \times 10^{-4}$  bar. The exact partial pressure of  $\text{O}_2$  was determined by measuring the equilibrium temperature of the reversible reaction (1) under the same atmosphere as that used in each experiment with  $\text{CuAl}_2\text{O}_4$ . The stabilised CuO-based particles have been characterised in previous work.<sup>24</sup> Some samples of  $\text{CuAl}_2\text{O}_4$  with higher masses,  $\sim 60$  mg each, were treated using a combination of the above protocols (with some variations in duration or gas composition, when necessary) to investigate the redox behaviour of the material further. Identification of the solid phases present in some of the recovered samples was also performed using XRD. The details of the changes made to the TG protocols will be specified along with the results in the next section.

### 3. Results

#### 3.1. The effect of different alumina precursors on the formation of $\text{CuAl}_2\text{O}_4$

The formation of  $\text{CuAl}_2\text{O}_4$  was found to occur at different temperatures, depending on the form of alumina (or precursor) used.  $\alpha$ -Alumina did not react appreciably with CuO at 900  $^{\circ}\text{C}$ , even after four repetitions of milling and calcination for 6 hours on the same sample, as confirmed by the absence of peaks belonging to  $\text{CuAl}_2\text{O}_4$  in the XRD diffractograms shown in Fig. 1. However, when calcined in air at the higher temperature of 1000  $^{\circ}\text{C}$  for 6 hours, a significant amount of  $\text{CuAl}_2\text{O}_4$  was formed and further milling and calcining led to the formation of  $\text{CuAlO}_2$  with almost all the free alumina consumed by the 4<sup>th</sup> calcination. When calcined at 950  $^{\circ}\text{C}$ , a small amount of  $\text{CuAl}_2\text{O}_4$  but no  $\text{CuAlO}_2$  was detected in the material. This observation is in agreement with the finding of Jacob and

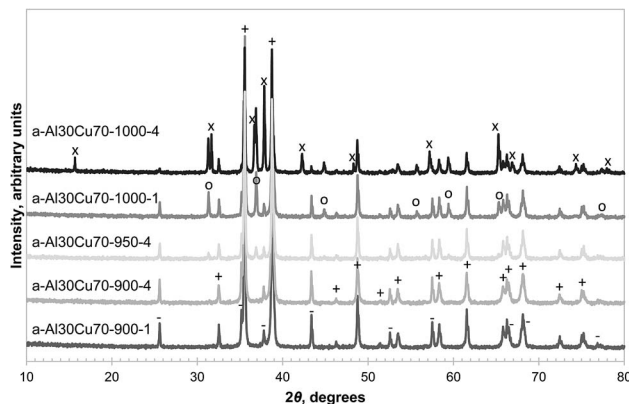


Fig. 1 XRD diffractograms of selected fresh samples prepared from  $\alpha$ -alumina with the major reflection peaks annotated as: CuO (+),  $\alpha$ - $\text{Al}_2\text{O}_3$  (–),  $\text{CuAl}_2\text{O}_4$  (O),  $\text{CuAlO}_2$  (x).

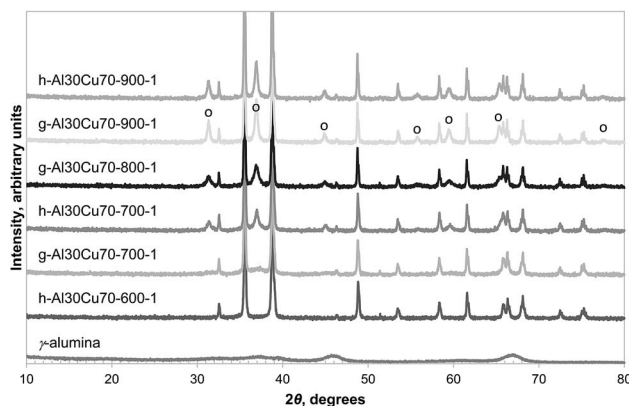


Fig. 2 XRD diffractograms of selected fresh samples prepared from  $\gamma$ -alumina and  $\text{Al}(\text{OH})_3$ . The reflection peaks of  $\text{CuAl}_2\text{O}_4$  are annotated (O) and the remaining peaks are due to CuO, with the exception of the  $\gamma$ -alumina sample at the bottom of the figure.

Alcock that in an atmosphere with  $P_{\text{O}_2} = 0.21$  bar, reaction (4) has an equilibrium temperature of 1003  $^{\circ}\text{C}$ .<sup>14</sup>

In contrast, Fig. 2 shows that, after heating in air at 850  $^{\circ}\text{C}$  for 6 hours, the formation of  $\text{CuAl}_2\text{O}_4$  from  $\gamma$ -alumina and CuO was significant. Since  $\gamma$ -alumina is only weakly reflecting and therefore difficult to quantify by XRD, the conversion of alumina to  $\text{CuAl}_2\text{O}_4$  was determined by measuring the changes in mass of a sample in a TGA at 900  $^{\circ}\text{C}$ , exposed successively to air,  $\text{N}_2$ ,  $\text{H}_2$  and finally air. As an example, the result for g-Al30Cu70-900-1 is shown in Fig. 3. It can be seen that the CLOU capacity of g-Al30Cu70-900-1 was  $\sim 5.3$  wt% and the total oxygen capacity of the material was 14.5 wt%, corresponding to a Cu content of 72.5 wt% on a CuO basis, instead of the expected value of 70 wt%. The difference was probably owing to adsorbed moisture in the  $\gamma$ -alumina used during the initial preparation. During the decomposition under  $\text{N}_2$ , the material exhibited a fast reaction stage between 900 and 1300 s, followed by a very slow stage until the atmosphere was switched to  $\text{H}_2$ . As will be discussed in Section 3.2., the reduction of  $\text{CuAl}_2\text{O}_4$  to  $\text{CuAlO}_2$  in an inert environment *via* reaction (3) is extremely slow. Thus it is plausible that the first



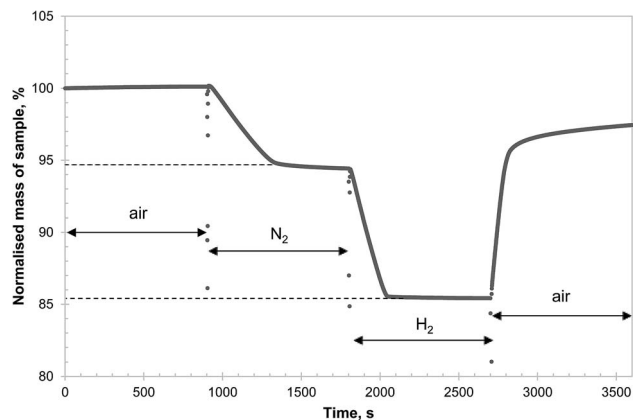


Fig. 3 TG curve of the isothermal reaction of g-Al30Cu70-900-1 in different atmospheres at 900 °C. The abrupt changes in mass seen between different segments were due to gas switching, disturbing the microbalance.

stage is dominated by reaction (1) and the second stage by the slow reaction (3). In fact, the chemical kinetics of decomposition of CuO in N<sub>2</sub> is faster than that being measured in this experiment<sup>24</sup> and here the rate is primarily limited by mass transfer in the TGA. A more detailed discussion is presented in the ESI.† The amount of free CuO present in g-Al30Cu70-900-1, which amounts to 52.8 wt%, can be estimated from the mass change during the fast stage. Assuming all remaining Cu is bound in the form of CuAl<sub>2</sub>O<sub>4</sub>, 91.8% of the  $\gamma$ -alumina present initially would have had to have been consumed during the calcination when the material was first prepared. The same analysis carried out on a sample of a-Al30Cu70-950-4 showed that only 2.4% of the  $\alpha$ -alumina had reacted during its preparation, albeit the material having been calcined at a higher temperature of 950 °C for a period 4 times longer.

Amongst the three precursors investigated, Al(OH)<sub>3</sub> was found to be the most reactive, capable of forming CuAl<sub>2</sub>O<sub>4</sub> at temperatures as low as 700 °C, as seen in Fig. 2. It should be noted that the Al(OH)<sub>3</sub> used in this work was amorphous, as confirmed by XRD (shown in Fig. S1 in the ESI†), as was the sample dehydrated at 600 °C for 24 hours. A small amount of  $\gamma$ -alumina was formed after Al(OH)<sub>3</sub> was calcined in air at 700 °C for 6 hours. Further characterisation of the Al(OH)<sub>3</sub> sample was undertaken using temperature programmed decomposition (TPD) in air in the TGA, with a heating rate of 2 °C min<sup>-1</sup>. The result is shown in Fig. 4. It can be seen that the hydroxide gradually lost H<sub>2</sub>O until ~600 °C and a marked decomposition occurred around 800 °C. It has been reported that amorphous alumina transforms to  $\gamma$ -alumina at 802 °C and subsequently to  $\alpha$ -alumina at 1087 °C.<sup>25</sup> In fact, when a sample of Al(OH)<sub>3</sub> was calcined at 900 °C in air for 6 hours, the resulting material was confirmed as  $\gamma$ -alumina (as shown in Fig. S1 in the ESI†). These results suggest that amorphous alumina is able to retain some OH groups up to 800 °C, which are lost when the phase transition to  $\gamma$ -alumina occurs.

### 3.2. The thermal decomposition of CuAl<sub>2</sub>O<sub>4</sub>

CuAl<sub>2</sub>O<sub>4</sub> was synthesised from the decomposition of nitrate precursors because (i) aluminium nitrate forms amorphous

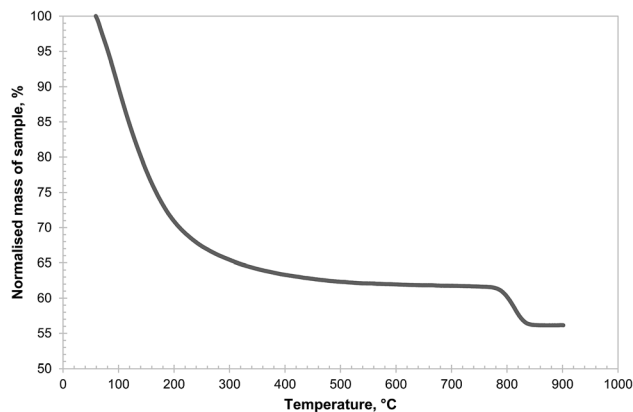


Fig. 4 Temperature programmed decomposition of Al(OH)<sub>3</sub> sample in air, using the TGA. A constant heating rate of 2 °C min<sup>-1</sup> was used and the mass of solid remaining at 900 °C was 56.1 wt%, in line with the material specification.

alumina on heating<sup>26</sup> and (ii) the gel method used ensured that the Cu and Al precursors were homogeneously mixed before firing at 1000 °C. XRD analysis, given in Fig. 5, confirmed that the synthesised sample was comprised primarily of CuAl<sub>2</sub>O<sub>4</sub> with trace amounts of CuO and  $\alpha$ -alumina. The decomposition of CuAl<sub>2</sub>O<sub>4</sub> in Ar at 900 °C, shown in Fig. S2 of the ESI,† was found to be slow and was not complete even after 20 hours. On the other hand, a similar degree of conversion was achieved in 50 minutes when the material was decomposed at 1000 °C, and the results are given in Fig. S3 of the ESI.† Based on these limited data of the isothermal decomposition, it appears that a high activation energy is associated with the reaction. Assuming the decomposition is due to reaction (3) alone, an apparent activation energy of the reaction can be estimated knowing the rate of change of conversion of the solid at various iso-conversion points (the procedure is briefly described in the ESI†). These values are plotted in Fig. S4 of the ESI,† up to a conversion of 0.8. The values were found to be fairly constant at ~370 kJ mol<sup>-1</sup> between conversions of 0.25 and 0.75. At lower values of conversion, the apparent activation energy was much

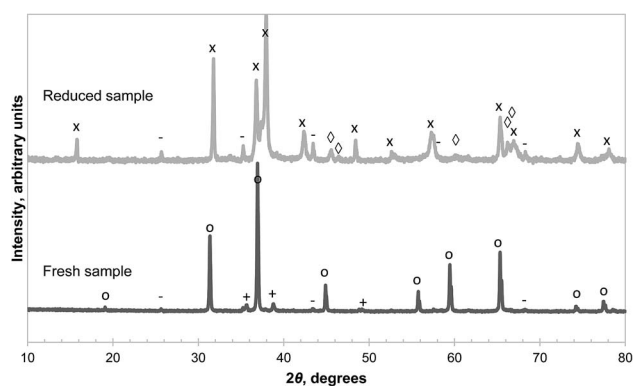


Fig. 5 XRD diffractograms of synthesised CuAl<sub>2</sub>O<sub>4</sub> as prepared (bottom) and after being decomposed in Ar at 900 °C for 20 hours (top). The major reflection peaks are annotated as: CuO (+),  $\alpha$ -Al<sub>2</sub>O<sub>3</sub> (-), CuAl<sub>2</sub>O<sub>4</sub> (O), CuAlO<sub>2</sub> (x),  $\gamma$ -Al<sub>2</sub>O<sub>3</sub> (◇).



lower. It may be possible that in the early stage of the decomposition, the rate-determining step is different from that at a later stage but this cannot be ascertained with the current data and further investigation is beyond the scope of this paper. It is worth noting that for a gas–solid reaction like reaction (3), the enthalpy of reaction is a measure of how fast the thermodynamic driving force changes with temperature in an inert gas atmosphere. Here, the apparent activation energy was found to be much higher than the enthalpy of reaction,  $\sim 140 \text{ kJ mol}^{-1}$ ,<sup>14</sup> suggesting that chemical kinetics has a larger effect than thermodynamics on the observed rate of reaction with changing temperature.

Examination of the reduced sample (recovered after decomposition at  $900^\circ\text{C}$  and cooled in Ar) revealed  $\text{CuAlO}_2$ ,  $\alpha$ -alumina and  $\gamma$ -alumina as the main phases present as seen in Fig. 5.  $\text{Cu}_2\text{O}$  was not detected in the reduced sample, contrary to the findings of Arjmand *et al.*,<sup>18</sup> who used  $\text{CH}_4$  instead of an inert gas. Interestingly, the reflections from  $\gamma$ -alumina are more consistent with a tetragonal structure, evident from the splitting of the peak around  $2\theta = 46^\circ$ , instead of the commonly-adopted cubic structure.<sup>27</sup> The phase obtained from the thermal decomposition of the synthetic  $\text{CuAl}_2\text{O}_4$  also appears to be more crystalline than the as-received  $\gamma$ -alumina, or that derived from amorphous alumina, the XRD diffractograms of which, given respectively in Fig. 2, and in Fig. S1 of the ESI,<sup>†</sup> contain much broader peaks. The amounts of various species present in the reduced sample were estimated by quantitative analysis of the XRD diffractogram and the results are shown in Table 1. The results are in good agreement with an independent estimate made from the thermogravimetric analysis, assuming that the unreacted sample consisted of pure  $\text{CuAl}_2\text{O}_4$  and the mass loss was due to the evolution of gaseous  $\text{O}_2$  according to reaction (3). The fact that a significant amount of  $\gamma$ -alumina was formed from the decomposition of  $\text{CuAl}_2\text{O}_4$  raises questions about the thermodynamics of reaction (3) because its standard Gibbs free energy of reaction at  $900^\circ\text{C}$  is reported as  $41.5 \pm 1.3 \text{ kJ mol}^{-1}$  (ref. 14) whereas the Gibbs free energy of transformation from  $\gamma$ -alumina to  $\alpha$ -alumina is approximately  $-14 \text{ kJ mol}^{-1}$  at the same temperature.<sup>28</sup> Consequently, the equilibrium  $P_{\text{O}_2}$  of reaction (3) would be rather different depending on the polymorph of the product alumina.

The results in Fig. 5 can be explained by two possible reaction schemes. In the first,  $\text{CuAl}_2\text{O}_4$  decomposes to both polymorphs of alumina in parallel, each having a different equilibrium  $P_{\text{O}_2}$ ; in the second,  $\text{CuAl}_2\text{O}_4$  decomposes to  $\gamma$ -

**Table 1** Amount of various species present in the sample of  $\text{CuAl}_2\text{O}_4$  reduced in Ar at  $900^\circ\text{C}$  for 20 hours

Species	Percentage by weight		Thermogravimetry
	XRD analysis		
$\text{CuAl}_2\text{O}_4$	12.8%		12.2%
$\text{CuAlO}_2$	65.5%		62.0%
$\gamma$ -Alumina	7.7%	21.7%	
$\alpha$ -Alumina	14.0%		25.8%

alumina first, which then transforms to  $\alpha$ -alumina. Further investigations were carried out to distinguish between the two schemes and the results are presented in Fig. 6. From the figure, it can be seen that the initial mass loss (over 160 s) of  $\text{CuAl}_2\text{O}_4$  when decomposed at  $1000^\circ\text{C}$  in  $P_{\text{O}_2}$  up to 0.02 bar showed two distinct linear regimes. The change of the average rate of mass loss with respect to  $P_{\text{O}_2}$  was significantly faster when  $P_{\text{O}_2} < 0.009$  bar. This result supports the hypothesis that the decomposition of  $\text{CuAl}_2\text{O}_4$  to the two forms of alumina occurs in parallel. Had the reaction followed the sequence  $\text{CuAl}_2\text{O}_4 \rightarrow \gamma$ -alumina  $\rightarrow \alpha$ -alumina, one would not expect such sudden change in the rate of decomposition with respect to  $P_{\text{O}_2}$ . As the decomposition proceeded rather slowly, external mass transfer did not have a significant influence on the measured rate of reaction: the estimated difference of  $P_{\text{O}_2}$  between the surface of the samples and that above the crucible holding the sample (4.9 mm diameter and 4 mm deep) using the fastest rate measured ( $\sim 0.135 \text{ mg}$  over 160 s, as shown in Fig. 6) was approximately  $1.5 \times 10^{-5}$  bar. Thus, assuming that the rate of decomposition of  $\text{CuAl}_2\text{O}_4$  was proportional to the difference between  $P_{\text{O}_2}$  of the gas environment and the equilibrium value, the equilibrium  $P_{\text{O}_2}$  of the two parallel reactions can be estimated from the intersection between the two regimes,  $8.7 \times 10^{-3}$  bar, and that between the slow regime and the abscissa, 0.034 bar. The difference in the equilibrium  $P_{\text{O}_2}$  amounts to a difference in the Gibbs free energy of  $14.4 \text{ kJ mol}^{-1}$  of reaction (3), assuming the activities of the solids are unity. However, this value is only  $\sim 60\%$  of the Gibbs free energy of transformation from  $\gamma$ -alumina to  $\alpha$ -alumina reported in the literature.<sup>28</sup> The discrepancy could be due to the tetragonal deformation of the  $\gamma$ -alumina having a lower Gibbs free energy of formation. In fact, at the temperature concerned, it is possible for  $\gamma$ -alumina to start transforming to other transition aluminas,<sup>29</sup> which is probably why a tetragonal deformation, rather than the more common cubic structure, was observed from the decomposition of  $\text{CuAl}_2\text{O}_4$ . On a side note, using the value of 0.034 bar, the Gibbs free energy of reaction (3) with  $\alpha$ -alumina as the product is estimated as  $35.6 \text{ kJ mol}^{-1}$ , slightly higher than the value of  $33.0$

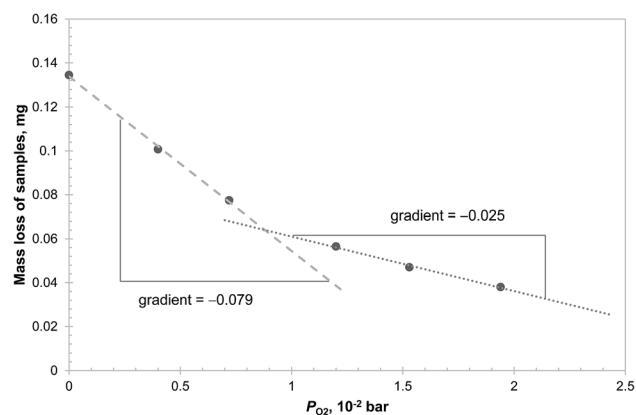


**Fig. 6** Loss of mass of samples of  $\text{CuAl}_2\text{O}_4$  during the initial 160 s of isothermal decomposition at  $1000^\circ\text{C}$  in different  $P_{\text{O}_2}$ . The mass of sample used in each experiment was between 19.46 mg and 19.67 mg.



$\text{kJ mol}^{-1}$ , given by Jacob and Alcock,<sup>14</sup> although the corresponding difference in  $P_{\text{O}_2}$  is more than 20%.

In addition, two samples of  $\text{CuAl}_2\text{O}_4$  were decomposed at  $1000\text{ }^\circ\text{C}$  in the TGA for 3 hours, one with  $P_{\text{O}_2} = 9.0 \times 10^{-3}$  bar, just above the transition point seen in Fig. 6, and the other in a mixture of  $\text{N}_2$  and Ar (where  $P_{\text{O}_2} < 5 \times 10^{-4}$  bar due to a small leakage of air into the TGA). The XRD diffractograms of the decomposed samples, given in Fig. 7, revealed that in the former case, some  $\text{CuAl}_2\text{O}_4$  remained but no  $\gamma$ -alumina was detected, whereas the converse is true for the latter. These observations also suggest that the decomposition of  $\text{CuAl}_2\text{O}_4$  to different phases of alumina probably occurs in parallel rather than in series.

### 3.3. The oxidation and reduction of $\text{CuAlO}_2$

There are two potential pathways for the oxidation of  $\text{CuAlO}_2$ , *i.e.* the backward reactions of (3) and (4). The equilibrium  $P_{\text{O}_2}$  of reaction (4) is significantly higher than that of reaction (3) in the temperature range of interest, between  $900\text{ }^\circ\text{C}$  and  $1000\text{ }^\circ\text{C}$ .<sup>14</sup> Therefore the two pathways can be examined separately by choosing an appropriate  $P_{\text{O}_2}$  so that only the backward reaction of (3) is thermodynamically feasible. Here, a sample of  $\text{CuAl}_2\text{O}_4$  was decomposed in a mixture of  $\text{N}_2$  and Ar at  $1000\text{ }^\circ\text{C}$  for 50 minutes, followed by oxidation in an atmosphere with  $P_{\text{O}_2} \approx 0.10$  bar (the equilibrium  $P_{\text{O}_2}$  of the reverse reaction (3) is  $\sim 0.04$  bar with  $\alpha$ -alumina as the reactant and that of reaction (4) is above 0.9 bar (ref. 14)) at the same temperature for a further 50 minutes and the result is shown in Fig. S6 of the ESI.† It was found that the oxidation of  $\text{CuAlO}_2$  *via* reaction (3) was much slower than the forward decomposition reaction, despite having a slightly higher thermodynamic driving force. The kinetics of the backward reaction (4) were not investigated in this work, as Arjmand *et al.* have shown previously that complete oxidation of  $\text{CuAlO}_2$  *via* this route was only achieved after prolonged heating in air.<sup>18</sup> It appears that both routes for the oxidation of  $\text{CuAlO}_2$

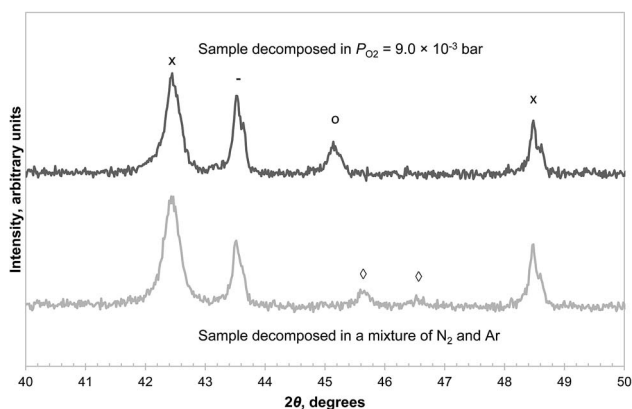


Fig. 7 XRD diffractograms of  $\text{CuAl}_2\text{O}_4$  decomposed at  $1000\text{ }^\circ\text{C}$  in different atmospheres. Only a section between  $2\theta = 40^\circ$  and  $50^\circ$  is shown to distinguish the peak due to  $\text{CuAl}_2\text{O}_4$  at  $45.2^\circ$  and that due to  $\gamma\text{-Al}_2\text{O}_3$  at  $45.6^\circ$ . The reflection peaks are annotated as  $\alpha\text{-Al}_2\text{O}_3$  (–),  $\text{CuAl}_2\text{O}_4$  (O),  $\text{CuAlO}_2$  (x),  $\gamma\text{-Al}_2\text{O}_3$  (◇). A separate graph containing the diffractograms between  $2\theta = 10^\circ$  and  $80^\circ$  can be found in the ESI (Fig. S5†).

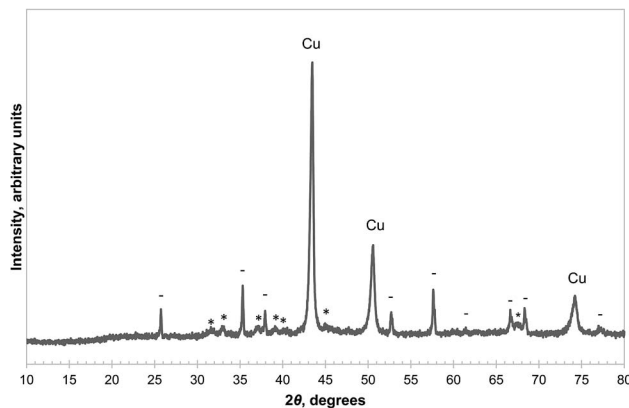


Fig. 8 XRD diffractograms of a sample of  $\text{CuAl}_2\text{O}_4$  first decomposed in 0.90%  $\text{O}_2$  at  $1000\text{ }^\circ\text{C}$  for 10 hours, then reduced by  $\text{H}_2$ . The annotations are: metallic Cu (Cu),  $\alpha\text{-Al}_2\text{O}_3$  (–),  $\theta$ -alumina (\*).

are slow and the material does not contribute to the oxygen carrying capacity significantly, bearing in mind that many chemical-looping processes oxidise the oxygen carrier in a circulating fluidised bed, which normally has a low residence time.

On the other hand, the reduction of  $\text{CuAlO}_2$  in  $\text{H}_2$  was fast. For instance, a sample of  $\text{CuAl}_2\text{O}_4$  first decomposed in an atmosphere with  $P_{\text{O}_2} = 9.0 \times 10^{-3}$  bar for 10 hours at  $1000\text{ }^\circ\text{C}$  was reduced completely in 5.5 minutes once the reactive gas was switched to 5%  $\text{H}_2$ . The average rate of loss of mass during this time was approximately  $0.6\text{ mg min}^{-1}$ . This is equivalent to  $38\text{ }\mu\text{mol min}^{-1}$  of oxygen atoms, and is comparable to the rate of transfer of  $\text{H}_2$  to the solid estimated in previous work for the same experimental arrangement, *i.e.* the reaction was limited by mass transfer.<sup>23</sup> XRD analysis of the reduced sample showed that the phases present were metallic Cu,  $\theta$ -alumina and  $\alpha$ -alumina, as annotated in Fig. 8. Several studies<sup>30–32</sup> suggest that the reduction of  $\text{CuAlO}_2$  at around  $1000\text{ }^\circ\text{C}$  results in interspersed Cu and  $\theta$ -alumina without any  $\alpha$ -alumina being formed. The  $\alpha$ -alumina present in this work is probably the result of the decomposition of  $\text{CuAl}_2\text{O}_4$  only and this is supported by a subsequent TG experiment, which is shown in Fig. 9 and will be discussed later. However, no attempt was made to synthesise pure  $\text{CuAlO}_2$  to confirm this, it not being the primary focus of the current work.

## 4. Discussion

The results presented in this work concur with previous findings that the generation of gas phase oxygen by the decomposition of the spinel phase,  $\text{CuAl}_2\text{O}_4$ , is slow up to  $1000\text{ }^\circ\text{C}$  (ref. 11 and 12) and therefore unsuitable for oxygen production schemes such as CLOU or CLAS. Thus, the formation of the spinel must be prevented to retain the high reactivity of  $\text{CuO}$  with regard to oxygen release. Since the typical operating temperature for the  $\text{CuO}/\text{Cu}_2\text{O}$  system is around  $900\text{ }^\circ\text{C}$ , it is viable to use  $\alpha$ -alumina as a support material but not amorphous alumina or  $\gamma$ -alumina, which react with  $\text{CuO}$  at much lower temperatures. Usually the latter two are preferred as



support materials since they possess much higher internal surface areas compared with  $\alpha$ -alumina. However, because the operating temperature is sufficiently high, a high surface area is not necessary to secure a high reaction rate and this has been demonstrated in previous work for various metal oxide oxygen carriers.<sup>6,23,33</sup> On the other hand, when high surface area is desired, *e.g.* for catalysis at intermediate or low temperatures, amorphous alumina and  $\gamma$ -alumina can be used as long as the operating temperature is below 600 °C and 700 °C, respectively, where the formation of  $\text{CuAl}_2\text{O}_4$  from CuO and respective alumina does not occur, as seen in Fig. 2. In any case, alumina supports should be avoided when the operating temperature is constantly above 950 °C since even the relatively-stable  $\alpha$ -alumina starts to form  $\text{CuAl}_2\text{O}_4$  at this temperature.

The fact that  $\text{CuAl}_2\text{O}_4$  decomposes to different polymorphs of alumina depending on the  $P_{\text{O}_2}$  of the environment can be exploited to regenerate the active CuO phase should the spinel be accidentally formed. The scheme is proposed as follows: first, the material containing the spinel phase would be maintained in an atmosphere with appropriate  $P_{\text{O}_2}$  (*e.g.* slightly above  $9.0 \times 10^{-3}$  bar if treated at 1000 °C, the transition point shown in Fig. 6) to slowly decompose the spinel into  $\alpha$ -alumina and the delafossite phase,  $\text{CuAlO}_2$ , while avoiding the formation of  $\gamma$ -alumina. Once the decomposition is complete, the material would be further reduced by a fuel gas (*e.g.*  $\text{CH}_4$  or syngas) at 900 °C or below, to minimise the sintering of the metallic Cu formed (the melting point of Cu is lower than its oxides, or the aluminates, at 1084 °C). The reduced material would then be re-oxidised to regenerate the CuO phase, preferably at low temperature and  $P_{\text{O}_2}$ , *e.g.*  $\sim 700$  °C and 0.01 bar, because

particles containing Cu agglomerate easily when being oxidised in air at high temperatures.<sup>9</sup>

To demonstrate the effectiveness of this procedure, a comparative study of  $\text{CuAl}_2\text{O}_4$  with different pre-treatments was performed in the TGA and the results are shown in Fig. 9. It can be seen from Fig. 9 that as-synthesised  $\text{CuAl}_2\text{O}_4$  (sample a) released a limited amount of oxygen in the first 15 minutes of the experiment and reducing the sample in  $\text{H}_2$  and re-oxidised once (sample b) did not bring significant improvement. However, the sample decomposed to  $\text{CuAlO}_2$  before being reduced in  $\text{H}_2$  (sample c) was able to release much more oxygen during the inert stage. All three samples were capable of being reduced completely in  $\text{H}_2$  and re-oxidised fully in air within minutes. The rates of reduction and oxidation were again limited by external mass transfer and did not reflect the reactivity of the materials. The slightly slower rates of reduction and oxidation observed for (sample c) were due to a slight increase in the flow rate of the purging Ar during this particular experiment, resulting in a higher dilution of the  $\text{H}_2$ , rather than the deactivation of the material. This was confirmed by identical rates of decomposition of the CuO observed for all materials during the decomposition in  $\text{N}_2$ , which is not affected by dilution of gases. Using the same analysis as undertaken in Fig. 3, it was estimated that approximately 6% of the Cu was present as CuO in sample (a) and the corresponding percentages in samples (b) and (c) were 23% and 55%, respectively. Assuming the additional CuO present in sample (c) arose entirely from the formation of  $\alpha$ -alumina (which does not reform  $\text{CuAl}_2\text{O}_4$  on subsequent oxidation), and that the decomposition of  $\text{CuAl}_2\text{O}_4$  to  $\text{CuAlO}_2$  produces  $\alpha$ -alumina exclusively, the expected amount of CuO in sample (c) would be 53% of the total Cu, very close to the value measured experimentally. In conjunction with results shown in Fig. 8, it can be inferred that the alumina formed from the reduction of  $\text{CuAlO}_2$  should be mostly, if not all, composed of the  $\theta$ -phase. Furthermore,  $\theta$ -alumina was able to react with the interspersed Cu to form  $\text{CuAl}_2\text{O}_4$  directly on oxidation without forming  $\text{CuAlO}_2$  as an intermediate—otherwise the oxidation would not have been complete. Owing to the presence of  $\theta$ -alumina, it would not be possible to recover all the Cu as CuO following the proposed protocol but 50% of the Cu bound in  $\text{CuAl}_2\text{O}_4$  could be recovered and if repeated several times, most of the Cu might be re-activated into the CuO phase.

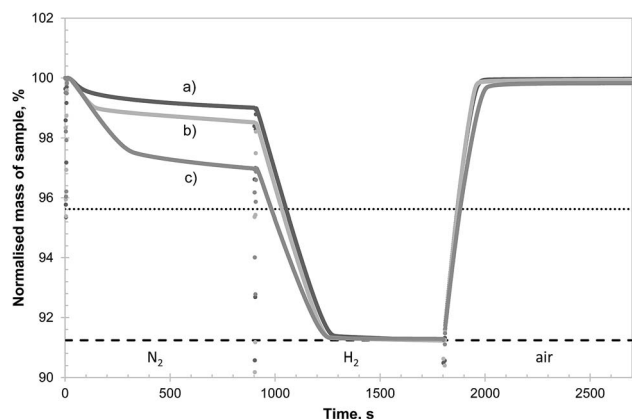


Fig. 9 TG curve of the isothermal reaction of 3 different samples of  $\text{CuAl}_2\text{O}_4$  in different atmospheres at 900 °C ( $\text{N}_2$ ,  $\text{H}_2$  and air). The samples were kept in air before the start of the experiment to maintain a fully oxidised state. The abrupt changes in mass seen between different segments were due to gas switching, disturbing the micro-balance. The dotted and dashed horizontal lines indicate, respectively, the theoretical mass change if all the  $\text{Cu}^{2+}$  present is reduced to  $\text{Cu}^+$  and metallic Cu. The 3 samples were: (a)  $\text{CuAl}_2\text{O}_4$  as synthesised (60.89 mg), (b)  $\text{CuAl}_2\text{O}_4$  fully reduced in  $\text{H}_2$  and re-oxidised in air at 900 °C prior to the experiment (61.37 mg) and (c)  $\text{CuAl}_2\text{O}_4$  first decomposed in 0.90%  $\text{O}_2$  at 1000 °C for 10 hours, then reduced by  $\text{H}_2$  (*i.e.* the same as in Fig. 8) followed by re-oxidation at 900 °C prior to experiment (61.11 mg).

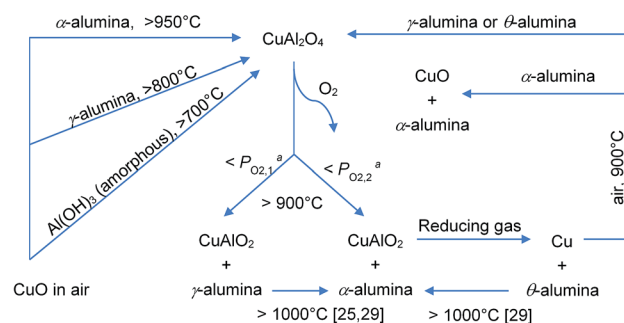


Fig. 10 Summary of possible reactions involving alumina and CuO and related compounds. <sup>a</sup> $P_{\text{O}_2,1} < P_{\text{O}_2,2}$ .



The series of interactions between CuO and alumina investigated in this work is summarised in Fig. 10.

## 5. Conclusion

The formation of  $\text{CuAl}_2\text{O}_4$  from CuO and alumina was investigated, together with its decomposition in an oxygen-lean environment. The oxidation and reduction characteristics of the related copper aluminate,  $\text{CuAlO}_2$ , was also studied. It was found that

(1) The solid–solid reaction between CuO and different polymorphs of alumina occurs at different temperatures. The ease of reaction follows the order amorphous alumina >  $\gamma$ -alumina >  $\alpha$ -alumina.

(2) It is possible to support CuO with  $\alpha$ -alumina for oxygen storage and production up to 950 °C without forming the undesired  $\text{CuAl}_2\text{O}_4$  phase, whereas aluminium hydroxide (and its derivative amorphous alumina),  $\gamma$ -alumina and  $\theta$ -alumina are unsuitable for this purpose.

(3)  $\text{CuAl}_2\text{O}_4$  can decompose slowly to form both  $\alpha$ -alumina and  $\gamma$ -alumina. By controlling the  $P_{\text{O}_2}$  of the environment, it is possible to bias the selectivity towards 100%  $\alpha$ -alumina so that on subsequent oxidation of the material, CuO could be formed instead of  $\text{CuAl}_2\text{O}_4$ .

(4)  $\text{CuAlO}_2$  resists oxidation in air but can be easily reduced in  $\text{H}_2$ .  $\theta$ -Alumina is formed in the reduction process.

(5) Based on the reactivity of  $\text{CuAl}_2\text{O}_4$  and  $\text{CuAlO}_2$ , a possible procedure for the regeneration of CuO from copper aluminates is proposed, which could recover up to 50% of the copper originally bound in the form of  $\text{CuAl}_2\text{O}_4$  in a single treatment.

## Acknowledgements

This work was supported by the Engineering and Physical Sciences Research Council (EPSRC Grants EP/I010912/1 and EP/K030132/1).

## References

- B. J. P. Buhre, L. K. Elliott, C. D. Sheng, R. P. Gupta and T. F. Wall, Oxy-fuel combustion technology for coal-fired power generation, *Prog. Energy Combust. Sci.*, 2005, **31**, 283–307, DOI: 10.1016/j.pecs.2005.07.001.
- M. B. Toftegaard, J. Brix, P. A. Jensen, P. Glarborg and A. D. Jensen, Oxy-fuel combustion of solid fuels, *Prog. Energy Combust. Sci.*, 2010, **36**, 581–625, DOI: 10.1016/j.pecs.2010.02.001.
- T. Mattisson, A. Lyngfelt and H. Leion, Chemical-looping with oxygen uncoupling for combustion of solid fuels, *Int. J. Greenhouse Gas Control*, 2009, **3**, 11–19, DOI: 10.1016/j.ijggc.2008.06.002.
- A. Abad, I. Adánez-Rubio, P. Gayán, F. García-Labiano, L. F. de Diego and J. Adánez, Demonstration of chemical-looping with oxygen uncoupling (CLOU) process in a 1.5 kWth continuously operating unit using a Cu-based oxygen-carrier, *Int. J. Greenhouse Gas Control*, 2012, **6**, 189–200, DOI: 10.1016/j.ijggc.2011.10.016.
- I. Adánez-Rubio, A. Abad, P. Gayán, L. F. de Diego, F. García-Labiano and J. Adánez, Biomass combustion with  $\text{CO}_2$  capture by chemical looping with oxygen uncoupling (CLOU), *Fuel Process. Technol.*, 2014, **124**, 104–114, DOI: 10.1016/j.fuproc.2014.02.019.
- I. Adánez-Rubio, A. Abad, P. Gayán, L. F. de Diego, F. García-Labiano and J. Adánez, Performance of CLOU process in the combustion of different types of coal with  $\text{CO}_2$  capture, *Int. J. Greenhouse Gas Control*, 2013, **12**, 430–440, DOI: 10.1016/j.ijggc.2012.11.025.
- B. Moghtaderi, Application of Chemical Looping Concept for Air Separation at High Temperatures, *Energy Fuels*, 2010, **24**, 190–198, DOI: 10.1021/ef900553j.
- L. F. de Diego, F. García-Labiano, J. Adánez, P. Gayán, A. Abad, B. M. Corbella and J. María Palacios, Development of Cu-based oxygen carriers for chemical-looping combustion, *Fuel*, 2004, **83**, 1749–1757, DOI: 10.1016/j.fuel.2004.03.003.
- L. F. de Diego, P. Gayán, F. García-Labiano, J. Celaya, A. Abad and J. Adánez, Impregnated  $\text{CuO}/\text{Al}_2\text{O}_3$  Oxygen Carriers for Chemical-Looping Combustion: Avoiding Fluidized Bed Agglomeration, *Energy Fuels*, 2005, **19**, 1850–1856, DOI: 10.1021/ef050052f.
- S. Chuang, J. Dennis, A. Hayhurst and S. Scott, Development and performance of Cu-based oxygen carriers for chemical-looping combustion, *Combust. Flame*, 2008, **154**, 109–121, DOI: 10.1016/j.combustflame.2007.10.005.
- M. Arjmand, A.-M. Azad, H. Leion, A. Lyngfelt and T. Mattisson, Prospects of  $\text{Al}_2\text{O}_3$  and  $\text{MgAl}_2\text{O}_4$ -Supported CuO Oxygen Carriers in Chemical-Looping Combustion (CLC) and Chemical-Looping with Oxygen Uncoupling (CLOU), *Energy Fuels*, 2011, **25**, 5493–5502, DOI: 10.1021/ef201329x.
- Q. Imtiaz, M. Broda and C. R. Müller, Structure–property relationship of co-precipitated Cu-rich,  $\text{Al}_2\text{O}_3$ - or  $\text{MgAl}_2\text{O}_4$ -stabilized oxygen carriers for chemical looping with oxygen uncoupling (CLOU), *Appl. Energy*, 2014, **119**, 557–565, DOI: 10.1016/j.apenergy.2014.01.007.
- Q. Song, W. Liu, C. D. Bohn, R. N. Harper, E. Sivaniah, S. A. Scott and J. S. Dennis, A high performance oxygen storage material for chemical looping processes with  $\text{CO}_2$  capture, *Energy Environ. Sci.*, 2013, **6**, 288–298, DOI: 10.1039/c2ee22801g.
- K. T. Jacob and C. B. Alcock, Thermodynamics of  $\text{CuAlO}_2$  and  $\text{CuAl}_2\text{O}_4$  and Phase Equilibria in the System  $\text{Cu}_2\text{O}$ – $\text{CuO}$ – $\text{Al}_2\text{O}_3$ , *J. Am. Ceram. Soc.*, 1975, **58**, 192–195, DOI: 10.1111/j.1151-2916.1975.tb11441.x.
- S. K. Misra and A. C. D. Chaklader, The System Copper Oxide–Alumina, *J. Am. Ceram. Soc.*, 1963, **46**, 509, DOI: 10.1111/j.1151-2916.1963.tb13788.x.
- P. Cho, T. Mattisson and A. Lyngfelt, Comparison of iron-, nickel-, copper- and manganese-based oxygen carriers for chemical-looping combustion, *Fuel*, 2004, **83**, 1215–1225, DOI: 10.1016/j.fuel.2003.11.013.
- Q. Imtiaz, A. M. Kierzkowska and C. R. Müller, Coprecipitated, copper-based, alumina-stabilized materials for carbon dioxide capture by chemical looping



- combustion, *ChemSusChem*, 2012, **5**, 1610–1618, DOI: 10.1002/cssc.201100694.
- 18 M. Arjmand, A.-M. Azad, H. Leion, T. Mattisson and A. Lyngfelt, Evaluation of  $\text{CuAl}_2\text{O}_4$  as an Oxygen Carrier in Chemical-Looping Combustion, *Ind. Eng. Chem. Res.*, 2012, **51**, 13924–13934, DOI: 10.1021/ie300427w.
- 19 I. Adánez-Rubio, P. Gayán, A. Abad, L. F. de Diego, F. García-Labiano and J. Adánez, Evaluation of a Spray-Dried  $\text{CuO}/\text{MgAl}_2\text{O}_4$  Oxygen Carrier for the Chemical Looping with Oxygen Uncoupling Process, *Energy Fuels*, 2012, **26**, 3069–3081, DOI: 10.1021/ef3002229.
- 20 M. Arjmand, M. Keller, H. Leion, T. Mattisson and A. Lyngfelt, Oxygen Release and Oxidation Rates of  $\text{MgAl}_2\text{O}_4$ -Supported  $\text{CuO}$  Oxygen Carrier for Chemical-Looping Combustion with Oxygen Uncoupling (CLOU), *Energy Fuels*, 2012, **26**, 6528–6539, DOI: 10.1021/ef3010064.
- 21 P. Gayán, I. Adánez-Rubio, A. Abad, L. F. de Diego, F. García-Labiano and J. Adánez, Development of Cu-based oxygen carriers for Chemical-Looping with Oxygen Uncoupling (CLOU) process, *Fuel*, 2012, **96**, 226–238, DOI: 10.1016/j.fuel.2012.01.021.
- 22 L. Xu, J. Wang, Z. Li and N. Cai, Experimental Study of Cement-Supported  $\text{CuO}$  Oxygen Carriers in Chemical Looping with Oxygen Uncoupling (CLOU), *Energy Fuels*, 2013, **27**, 1522–1530, DOI: 10.1021/ef301969k.
- 23 F. Donat, W. Hu, S. A. Scott and J. S. Dennis, Characteristics of Copper-based Oxygen Carriers Supported on Calcium Aluminates for Chemical-Looping Combustion with Oxygen Uncoupling (CLOU), *Ind. Eng. Chem. Res.*, 2015, **54**, 6713–6723, DOI: 10.1021/acs.iecr.5b01172.
- 24 W. Hu, F. Donat, S. A. Scott and J. S. Dennis, Kinetics of oxygen uncoupling of a copper based oxygen carrier, *Appl. Energy*, 2016, **161**, 92–100, DOI: 10.1016/j.apenergy.2015.10.006.
- 25 F. Abbattista, S. Delmastro, G. Gozzelino, D. Mazza, M. Vallino, G. Busca, V. Lorenzelli and G. Ramis, Surface characterization of amorphous alumina and its crystallization products, *J. Catal.*, 1989, **117**, 42–51, DOI: 10.1016/0021-9517(89)90219-4.
- 26 B. Pacewska and M. Keshr, Thermal transformations of aluminium nitrate hydrate, *Thermochim. Acta*, 2002, **385**, 73–80, DOI: 10.1016/s0040-6031(01)00703-1.
- 27 G. Paglia, C. E. Buckley, A. L. Rohl, B. A. Hunter, R. D. Hart, J. V. Hanna and L. T. Byrne, Tetragonal structure model for boehmite-derived  $\gamma$ -alumina, *Phys. Rev. B: Condens. Matter Mater. Phys.*, 2003, **68**, 144110, DOI: 10.1103/physrevb.68.144110.
- 28 M. Chase, *Nist-Janaf thermochemical tables*, American Institute of Physics, Woodbury, New York, 1998.
- 29 K. Wefers and C. Misra, Oxides and Hydroxides of Aluminum, *Alcoa Tech. Pap.*, 19, 1987, pp. 1–100, [http://www.alcoa.com/global/en/innovation/papers\\_patents/pdf/TP19\\_Wefers.pdf](http://www.alcoa.com/global/en/innovation/papers_patents/pdf/TP19_Wefers.pdf), accessed 12 July, 2016.
- 30 M. Kracum, A. Kundu, M. P. Harmer and H. M. Chan, Novel interpenetrating  $\text{Cu}-\text{Al}_2\text{O}_3$  structures by controlled reduction of bulk  $\text{CuAlO}_2$ , *J. Mater. Sci.*, 2014, **50**, 1818–1824, DOI: 10.1007/s10853-014-8744-8.
- 31 D. Byrne, A. Cowley, P. McNally and E. McGlynn, Delafossite  $\text{CuAlO}_2$  film growth and conversion to  $\text{Cu}-\text{Al}_2\text{O}_3$  metal ceramic composite *via* control of annealing atmospheres, *CrystEngComm*, 2013, **15**, 6144, DOI: 10.1039/c3ce40197a.
- 32 Z. Yu, M. Kracum, A. Kundu, M. P. Harmer and H. M. Chan, Microstructural Evolution of a Cu and  $\theta\text{-Al}_2\text{O}_3$  Composite Formed By Reduction of Delafossite  $\text{CuAlO}_2$ : A HAADF-STEM Study, *Cryst. Growth Des.*, 2016, **16**, 380–385, DOI: 10.1021/acs.cgd.5b01362.
- 33 C. Linderholm, A. Lyngfelt, A. Cuadrat and E. Jerndal, Chemical-looping combustion of solid fuels – operation in a 10 kW unit with two fuels, above-bed and in-bed fuel feed and two oxygen carriers, manganese ore and ilmenite, *Fuel*, 2012, **102**, 808–822, DOI: 10.1016/j.fuel.2012.05.010.

